Comparative Study of the Thermoelectric Properties of Amorphous $Zn_{41}Sb_{59}$ and Crystalline Zn_4Sb_3

Yang Wu,[†] Johanna Nylén,[†] Craig Naseyowma,[†] N. Newman,[‡] Francisco J. Garcia-Garcia,[§] and Ulrich Häussermann*,[†]

Department of Chemistry and Biochemistry, Arizona State University, P.O. Box 871604, Tempe, Arizona 85287−1604, School of Materials, Arizona State University, P.O. Box 876006, Tempe, Arizona 85287−6006, and Lehrstuhl für Festkörperchemie, Institut für Physik, Universität Augsburg, Universitätsstrasse 1, D-86159 Augsburg, Germany

Received October 23, 2008

The alloy $Zn_{41}Sb_{59}$ was synthesized by high-pressure techniques and its bulk amorphous nature at ambient conditions confirmed by X-ray powder diffraction and electron microscopy studies. Electrical resistivity, thermopower, and thermal conductivity of $Zn_{41}Sb_{59}$ were measured in a temperature range from 6 to 350 K. $Zn_{41}Sb_{59}$ is a semiconductor and resistivity data suggest an activation energy of about 0.25 eV above 250 K. The thermopower is positive and increases with increasing temperature. Room-temperature values for the resistivity and thermopower are 8 Ω cm and 300 μV/K, respectively. The temperature dependence of the thermal conductivity is characteristic for amorphous solids and continuously increasing from 0.08 W/(m K) at 6 K to 0.19 W/(m K) at room temperature. Comparison of the thermal conductivity of $Zn_{41}Sb_{59}$ with the thermal lattice conductivity of the crystalline thermoelectric material β-Zn_4Sb_3 reveals a remarkable resemblance, justifying the classification of the latter as a phonon-glass material.

1. Introduction

The binary Zn−Sb phase diagram offers puzzling intricacy in terms of complex structured, often temperature polymorphic, phases occurring in a range between 50 and 60 at % Zn.[1−9] Some of these phases are narrow-gap semiconductors and display interesting thermoelectric properties.[10,11] This holds especially true for β-Zn_4Sb_3, which is considered to be a state-of-the-art material at moderate temperatures (450−650 K).[12] Especially remarkable is the extraordinarily low thermal conductivity of β-Zn_4Sb_3 which is similar to vitreous materials. Recently, β-Zn_4Sb_3 was recognized as substantially disordered,[13,14] featuring vacancies and interstitial Zn atoms in its rhombohedral crystal structure, which provided a plausible explanation for the low thermal conductivity.

A further peculiarity of the Zn−Sb phase diagram is its high-pressure behavior. According to Russian researchers the ambient pressure phases Zn_3Sb_2, Zn_4Sb_3, and ZnSb become successively unstable and decompose.[15] At pressures above 7 GPa, only a crystalline metallic alloy phase $Zn_{41}Sb_{59}$ is stable.[16] Similar to the ambient pressure phases Zn_4Sb_3 and Zn_3Sb_2, high-pressure $Zn_{41}Sb_{59}$ appears to be temperature polymorphic. A low-temperature form (the γ-phase) with the simple hexagonal structure is obtained with room-temperature compression, whereas temperatures above 250 °C afford the δ-phase with a yet unknown structure.[17,18] The latter phase can be retained at ambient pressure if quenched at high pressures to liquid nitrogen temperature. Subsequent

* Corresponding author. E-mail: Ulrich.Haussermann@asu.edu.
† Department of Chemistry and Biochemistry, Arizona State University.
‡ School of Materials, Arizona State University.
§ Universität Augsburg.

(1) Izard, V.; Record, M. C.; Tedenac, J. C.; Fries, S. G. *CALPHAD* **2001**, *25*, 567.
(2) Almin, K. E. *Acta Chem. Scand.* **1948**, *2*, 400.
(3) (a) Ugai, Y. A.; Marshakova, T. A.; Shevchenko, V. Y.; Demina, N. P. *Izv. Akad. Nauk SSSR, Neorg. Mater.* **1969**, *5*, 1381. (b) Shevnchenko, V. Y.; Skriplin, V. A.; Ugai, Y. A.; Marshakova, T. A. *Izv. Akad. Nauk SSSR, Neorg. Mater.* **1968**, *4*, 139. (c) Ignatev, N. A.; Ugai, Y. A.; Aleinko, K. B.; Rabotkin, N. S. *Z. Strukt. Khim.* **1971**, *12*, 729.
(4) Mayer, H. W.; Mikhail, I.; Schubert, K. *J. Less-Common Met.* **1978**, *59*, 43.
(5) (a) Mozharivskyj, Y.; Pecharsky, A. O.; Bud'ko, S.; Miller, G. J. *Chem. Mater.* **2004**, *16*, 1580. (b) Mozharivskyj, Y.; Janssen, Y.; Harringa, J. L.; Kracher, A.; Tsokol, A. O.; Miller, G. J. *Chem. Mater.* **2006**, *18*, 822.
(6) Boström, M.; Lidin, S. *J. Alloys Compd.* **2004**, *376*, 49.
(7) Nylén, J.; Andersson, M.; Lidin, S.; Häussermann, U. *J. Am. Chem. Soc.* **2004**, *126*, 16306.
(8) Nylén, J.; Lidin, S.; Andersson, M.; Iversen, B. B.; Liu, H. X.; Newman, N.; Häussermann, U. *Chem. Mater.* **2007**, *19*, 834.
(9) Nylén, J.; Lidin, S.; Andersson, M.; Liu, H.; Newman, N.; Häussermann, U. *J. Solid State Chem.* **2007**, *180*, 2603.
(10) (a) Ugai, Y. A.; Averbakh, E. M.; Lavrov, V. V. *Sov. Phys.−Solid State* **1963**, *4*, 2393. (b) Ugai, Y. A.; Averbakh, E. M. *Sov.Phys.−Solid State* **1963**, *5*, 940.
(11) Shaver, P. J.; Blair, J. *Phys. Rev.* **1966**, *141*, 649.
(12) Caillat, T.; Fleurial, J.-P.; Borshchevsky, A. *J. Chem. Phys. Solids* **1997**, *58*, 1119.
(13) Snyder, G. J.; Christensen, M.; Nishibori, E.; Caillat, T.; Iversen, B. B. *Nat. Mater.* **2004**, *3*, 458.
(14) Cargnoni, F.; Nishibori, E.; Rabiller, P.; Bertini, L.; Snyder, G. J.; Christensen, M.; Gatti, C.; Iversen, B. B. *Chem.−Eur. J.* **2004**, *10*, 3861.
(15) Ponyatovsky, E. G.; Belash, I. T. *High Temp.−High Press.* **1977**, *9*, 645.
(16) Antonov, V. E.; Barkalov, O. I.; Fedotov, V. K.; Harkunov, A. I.; Kolyubakin, A. I.; Ponyatovsky, E. G.; Winzenick, M. *Phys. Rev. B* **2000**, *62*, 3130.
(17) Barkalov, O. I. *High Pressure Res.* **2003**, *3*, 317.
(18) Degtyareva, V. F.; Bdikin, I. K.; Khasanov, S. S. *Phys. Solid State* **1997**, *39*, 1341.

10.1021/cm802893v CCC: $40.75
Published on Web 12/09/2008

heating to room temperature transforms crystalline δ-$Zn_{41}Sb_{59}$ into an amorphous phase with the same composition (am-$Zn_{41}Sb_{59}$).[19]

Ideal thermoelectrics have been described as "phonon glass−electron crystal (PGEC)" materials[20] and structurally disordered (but crystalline) β-Zn_4Sb_3 has been discussed to approach PGEC conditions closely.[13] In this respect, am-$Zn_{41}Sb_{59}$ offers an interesting perspective to explore the PGEC paradigm of thermoelectrics when posing two fundamental questions: (a) How does the thermal conductivity of amorphous $Zn_{41}Sb_{59}$, providing a lower boundary for the lattice thermal conductivity of zinc antimony systems, relate to disordered, crystalline, β-Zn_4Sb_3? (b) How does the electrical conductivity of the amorphous materials relate to crystalline β-Zn_4Sb_3? That is, to what extent can a true amorphous material actually maintain "electron crystal" properties? In most instances, amorphous materials will be poor electrical conductors. However, some years ago, Nolas and Goldsmid proposed circumstances under which an amorphous semiconductor can attain promising thermoelectric properties.[21] Will they apply to am-$Zn_{41}Sb_{59}$? Although some transport properties of am-$Zn_{41}Sb_{59}$ were determined earlier,[22] they have not been discussed with respect to thermoelectricity or related to those of crystalline zinc antimonide phases. In this work, we report the synthesis of am-$Zn_{41}Sb_{59}$ and its thermoelectric property characterization comprising electrical resistivity, Seebeck coefficient, and thermal conductivity measurements and compare obtained results with Zn_4Sb_3.

2. Experimental Section

Sample Preparation and Characterization. β-Zn_4Sb_3 was prepared from a 4:3 Zn:Sb mixture of the pure elements, which was pressed into a pellet and heated to 923 K in an evacuated silica tube. After 12 h, the sample was slowly cooled (at a rate of 5 K/h) to 723 K and subsequently quenched in water. The product was obtained as a shiny ingot, which was analyzed by X-ray powder diffraction (Guinier camera, Cu Kα_1) and energy-dispersive X-ray spectroscopy in a JEOL 820 scanning electron microscope. It corresponded to single phase β-Zn_4Sb_3. For the preparation of am-$Zn_{41}Sb_{59}$ a mixture Zn:Sb = 41:59 of the pure elements was pressed into a pellet and heated to 923 K in an evacuated silica tube. After 12 h the sample was quenched in water. The product corresponding to a two-phase mixture ZnSb + Sb was then ground to a fine powder and placed in a boron nitride (BN) capsule (4.55 mm diameter, 2.55 mm long) being part of the high-pressure cell assembly. To complete the assembly, the BN capsule was positioned with a graphite furnace and a zirconia insulating sleeve in a magnesia octahedron with 14 mm edge length. See ref 23 for details. The sample was pressurized to 8 GPa in a 6−8 Walker-type multianvil high pressure device with tungsten carbide cubes truncated to 8 mm edge length. After reaching the target pressure the sample was heated to 773 K over a time of 15 min, kept at this temperature for 1 h and finally cooled to room temperature over a time of 1 h. The pressure was released and am-$Zn_{41}Sb_{59}$ recovered as a cylindrical shaped, dense rod (4.48 mm diameter, 2.48 mm length) with gray color. The composition of am-$Zn_{41}Sb_{59}$ was examined by microprobe analysis in a JEOL JXA-8600 microscope (operated at 15.0 kV and 30.0 nA; elemental Sb and Zn as standards) and its amorphous state confirmed by powder X-ray diffraction patterns taken on a Siemens D5000 diffractometer (Bragg−Brentano geometry; Cu Kα radiation) and electron microscopy studies.

Electron Microscopy Investigations. am-$Zn_{41}Sb_{59}$ specimens for electron microscopy studies were prepared by finely grinding a small piece of the rod obtained from the high-pressure experiment under ethanol. A drop of the resulting dispersion was put onto holey-carbon coated copper grids. These grids were examined in a JEOL JEM 2100F operated at 200 kV. Compositional analysis of the samples by X-ray energy-dispersive spectrometry was carried out with an EDAX detector attached to the transmission electron microscope (TEM). High-resolution images were recorded with a slow scan CCD camera (Gatan model UltraScan 1000) and electron diffraction patterns with a DITABIS imaging plate system.

Physical Property Measurements. The electrical resistivity (two-point probe configuration), thermopower and thermal conductivity of β-Zn_4Sb_3 and am-$Zn_{41}Sb_{59}$ were measured on a physical property measurement system (PPMS) from Quantum Design equipped with the thermal transport option (TTO). A piece from a fragmented β-Zn_4Sb_3 ingot with dimensions 2.50 × 2.50 × 3.40 mm and the as prepared am-$Zn_{41}Sb_{59}$ rod were polished and utilized as specimens. Two copper disks with extruded leads on each end were glued oppositely onto the specimen using a two-component silver-filled epoxy (Epo-Tek H20E), which provided contact after curing at slightly elevated temperatures for a short time. The arrangement was then mounted on the TTO puck, which was subsequently loaded into the PPMS chamber and then evacuated to high vacuum ($<1 \times 10^{-3}$ torr) for the measurement. The thermal transport measurements were conducted in a two-point configuration from 10 to 350 K at a scanning rate of 0.3 K/min for Zn_4Sb_3 and from 6 to 350 K at a scatting rate of 0.15 K/min for am-$Zn_{41}Sb_{59}$, respectively. The slower scanning rate applied to am-$Zn_{41}Sb_{59}$ was due to its quite low thermal conductivity, which required a longer equilibrating time for the steady state measurement. At a certain temperature, a heat pulse was applied to the sample to create a temperature disparity. Thermal conductivity and Seebeck coefficient were obtained when the sample was equilibrated. Resistivity was then acquired by introducing up to a maximum value of 1.5 mA AC current at a frequency of 17 Hz. The autorange feature was used in all of the measurements in the PPMS system. Radiation heat loss was automatically corrected with the incorporated functions of the software. For more accurately determining the resistivity of Zn_4Sb_3, another piece of the fragmented β-Zn_4Sb_3 ingot was prepared for a four-point probe in-line configuration measurement (dimension 1.10 × 1.25 × 1.50 mm), which was conducted on the same PPMS using its resistivity option. A constant current of 1 mA was supplied and the resistance was recorded in the same temperature range at a rate of 1 K/min. A four-point probe measurement of the resistivity was deemed necessary to estimate the lattice thermal conductivity of Zn_4Sb_3 from the Wiedemann−Franz relation. The two- and four-point probe measurements, however, gave very similar results.

3. Results and Discussion

The amorphous phase am-$Zn_{41}Sb_{59}$ has been previously prepared by "thermobaric quenching" where two-phase mixtures ZnSb + Sb with the composition $Zn_{41}Sb_{59}$ were

(19) Belash, I. T.; Degtyareva, V. F.; Ponyatovsky, E. G.; Rashupkin, V. I. *Sov. Solid State Phys.* **1987**, *6*, 1788.
(20) SlackG. A. *CRC Handbook of Thermoelectrics*; Rowe, D. M., Ed.; CRC Press: Boca Raton, FL, 1995; p 407.
(21) Nolas, G. S.; Goldsmit, H. J. *Phys. Status Solidi A* **2002**, *194*, 271.
(22) (a) Antonov, V. E.; Barkalov Kolyubakin, A. I. *J. Non-Cryst. Solids* **1994**, *176*, 58. (b) Antonov, V. E.; Barkalov, O. I.; Kolyubakin, A. I.; Ponyatovsky, E. G. *Phys. Status Solidi B* **1996**, *198*, 497.
(23) Leinenweber, K.; Parise, J. *J. Solid State Chem.* **1995**, *114*, 277.

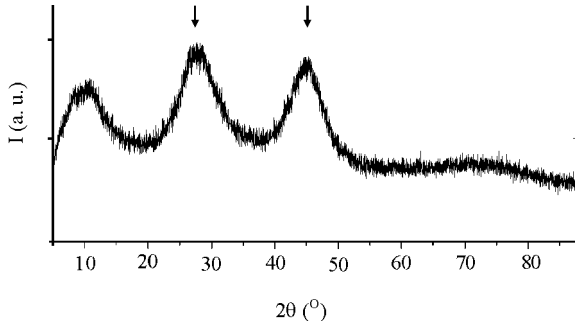

Figure 1. X-ray diffraction pattern (Cu Kα radiation) of am-$Zn_{41}Sb_{59}$. Arrows mark halos at $d \approx 2.0$ Å and $d \approx 3.2$ Å.

subjected to 7.5 GPa and 600 K for 24 h and subsequently quenched to 100 K.[24] This pressure-temperature treatment produces a crystalline high-pressure δ-phase that is stable at $P > 6.5$ GPa and metastable at ambient pressure and low temperatures. Heating to room temperature causes the δ-phase to transform into am-$Zn_{41}Sb_{59}$. In our synthesis, the starting mixture ZnSb + Sb was heated to 773 K for 1 h at 8 GPa and then cooled to room temperature over a period of 1 h, after which the pressure was released. This procedure affords directly am-$Zn_{41}Sb_{59}$, presumably via intermediate γ or δ-phase. We found that slow cooling affords a homogenously amorphous sample, while samples quenched from 773 K to room temperature contained various amounts of crystalline inclusions with sizes ranging from 2 to 6 nm. According to TEM-EDX analysis, these inclusions contain both Zn and Sb and may correspond to the δ-phase. Electron probe microprobe analysis show that the composition of am-$Zn_{41}Sb_{59}$ is close to 41:59 (40.3(8) at % Zn, 59.7(7) at % Sb). When employing more Zn- or Sb-rich mixtures as starting material in the high-pressure synthesis, samples consist of am-$Zn_{41}Sb_{59}$ and segregated crystalline Zn and Sb, respectively. Upon heating to about 450 K, am-$Zn_{41}Sb_{59}$ transforms to crystalline ZnSb and amorphous Sb.[24]

The X-ray diffraction pattern of am-$Zn_{41}Sb_{59}$ is shown in Figure 1 and displays two halos with maxima around $2\theta = 27.5$ and 40.0° corresponding to $d = 3.4$ and 2.0 Å, respectively. This is in agreement with an earlier neutron diffraction study of am-$Zn_{41}Sb_{59}$ where the two first maxima of the structure factor are located around $Q = 3.4$ and 2.0 Å.[25] am-$Zn_{41}Sb_{59}$ was further subjected to an electron microscopy investigation. Because the thermal stability of the sample is rather low, the integrity of particles under the electron beam needed to be determined. Taking advantage of the high sensibility and dynamical range of imaging plates a series of electron diffraction patterns at different electron radiation exposures and time was recorded. Diffraction patterns at increasingly high intensity showed the same details and no changes were observed. Thus, we could conclude that am-$Zn_{41}Sb_{59}$ particles are perfectly stable under the electron beam and confirm that the contrast observed in the high resolution images show the real amorphous atomic

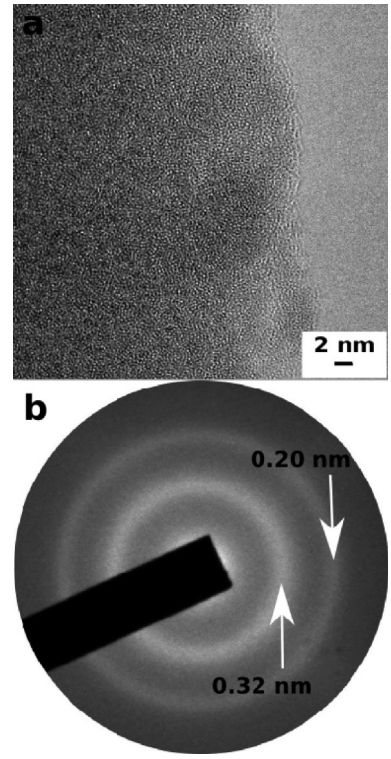

Figure 2. (a) High-resolution image of an am-$Zn_{41}Sb_{59}$ particle. The observed contrast represents the amorphous atomic structure. (b) Corresponding electron diffraction pattern. The spacings for the observed rings of diffracted intensity are indicated.

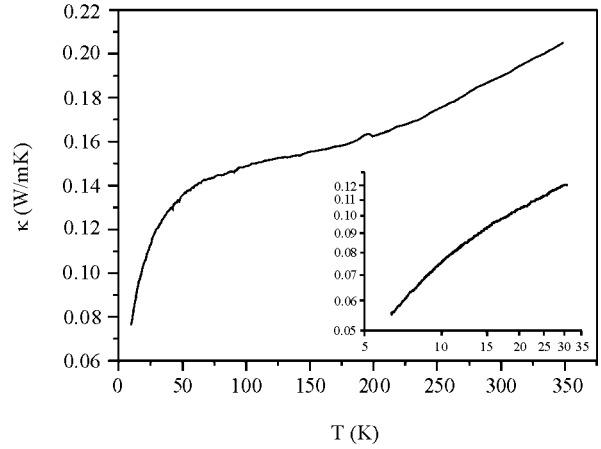

Figure 3. Thermal conductivity κ of am-$Zn_{41}Sb_{59}$. The inset is a blow up of the low-temperature region (log κ vs log T).

structure as seen in Figure 2. The corresponding electron diffraction pattern displays two rings of intensity. The associated spacing is in agreement with the X-ray diffraction pattern.

The thermal conductivity κ of am-$Zn_{41}Sb_{59}$ is displayed in Figure 3. In amorphous materials κ decreases with decreasing temperature at all temperatures.[26] Frequently a plateau occurs between about 20 and 1 K, followed by a sharp drop when entering the low temperature region ($T <$ 1 K). Such a plateau behavior is not observed for am-$Zn_{41}Sb_{59}$ for $T > 6$ K (it may occur at even lower temperatures), but instead κ follows closely a behavior

(24) Ponyatovsky, E. G.; Barkalov, O. I. *Mater. Sci. Eng., A* **1991**, *133*, 726.
(25) Barkalov, O. I.; Kolesnikov, A. I.; Ponyatovsky, E. G; Dahlborg, U.; Delaplane, R; Wannberg, A. *J. Non-Cryst. Solids* **1994**, *176*, 263.
(26) Tritt, T. M., Ed. *Thermal Conductivity: Theory, Properties and Applications*; Springer: New York, 2004.

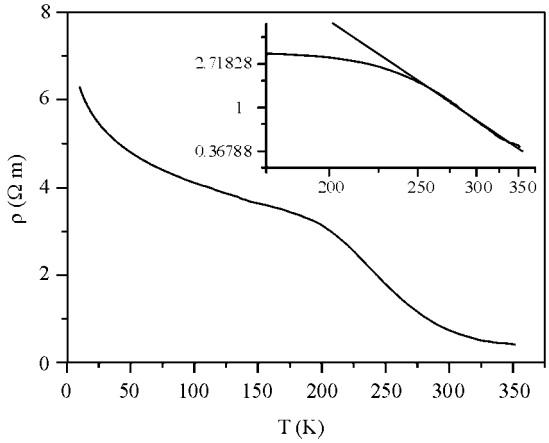

Figure 4. Electrical resistivity ρ of am-$Zn_{41}Sb_{59}$ (two-point probe measurement). The inset shows the Arrhenius behavior of ρ for temperatures above 250 K.

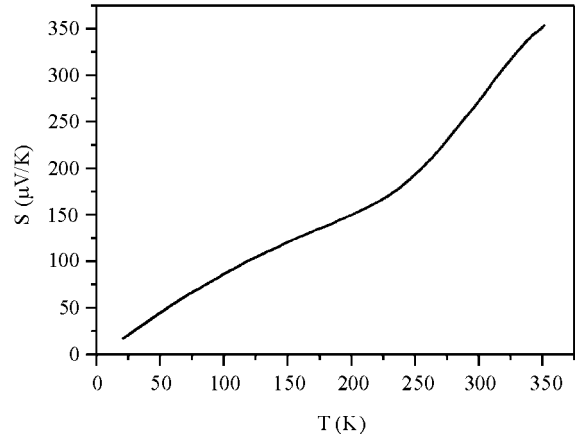

Figure 5. Thermopower S of am-$Zn_{41}Sb_{59}$.

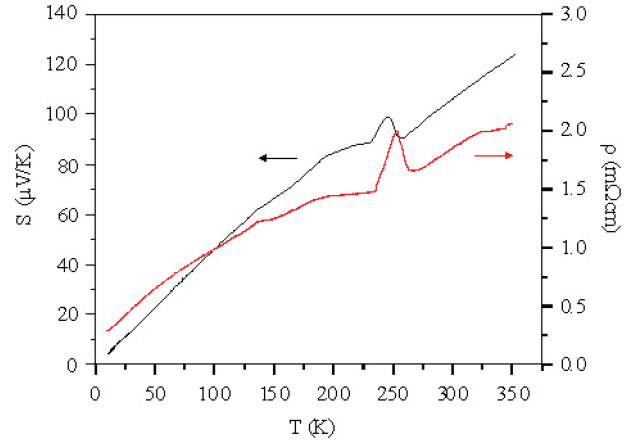

Figure 6. Thermopower S (black line) and electrical resistivity ρ (red line, four-point probe measurement) of Zn_4Sb_3.

expected from the concept of minimum thermal conductivity which assumes heat transfer in random walks between neighboring atoms behaving as strongly damped localized oscillators.[27] The temperature dependence of the thermal conductivity of amorphous solids is usually not very dependent on the composition, whereas magnitudes may vary by one order. In this respect, the thermal conductivity am-$Zn_{41}Sb_{59}$ increases by about 50% in the temperature range 100−350 K, from 0.15 to 0.21 W/(m K), which compares well with the behavior of, for example, vitreous silica. However, κ magnitudes for the latter material are about five times higher.[26]

The electrical resistivity ρ of am-$Zn_{41}Sb_{59}$ shows semiconductor behavior and decreases with increasing temperature over the whole investigated temperature range (Figure 4). Around 200 K, a discontinuous drop is seen, and above 250 K the temperature dependence of ρ follows an Arrhenius behavior with an activation energy of about 0.24 eV. We note that the high temperature behavior of our sample is roughly in agreement with a previous resistivity measurement of am-$Zn_{41}Sb_{59}$ by Antonov et al.[22] However, in the earlier measurement, which was performed between 120 and 370 K, Arrhenius behavior (with an activation energy of 0.3 eV) was found for the whole temperature range and consequently very high resistivity values (approaching 1×10^6 Ω m) were obtained at low temperatures. Even more dramatic is the discrepancy in the thermopower S between our measurement and ref 22. Antonov et al. report a negative temperature dependence where values exceed 1100 μV/K at 200 K and decrease to below 700 μV/K at 370 K. According to our measurement the positive thermopower increases almost linearly from 10 μV/K at 10 K to 370 μV/K at 350 K (Figure 5). A kink occurs around 225 K, which probably relates to the resistivity change between Arrhenius and non-Arrhenius behavior. The reason for the discrepancy between our resistivity and thermopower measurements and the data obtained by Antonov et al. is not clear but may be related to the different sample preparation.

We now turn to the properties of Zn_4Sb_3. Figure 6 shows the temperature dependence of the resistivity and the thermopower in a range from 10 to 350 K. Both properties show pronounced discontinuities at around 255 and 235 K, where upon cooling Zn_4Sb_3 undergoes two phase transitions from room temperature stable, disordered, β-Zn_4Sb_3 to the consecutively higher ordered phases α and α′, respectively.[8,9] The α−α′ transition is triggered by a slight Zn deficiency of Zn_4Sb_3 with respect to its ideal crystallographic composition $Zn_{13}Sb_{10}$ ($Zn_{3.9}Sb_3$). As a matter of fact, at low temperatures, Zn_4Sb_3 corresponds to a two-phase mixture of α and α′ phase and the α−α′ transition can be thought of an internal disproportionation of $Zn_{13-\delta}Sb_{10}$ into an α phase with a slightly higher Zn content than that present between 235 and 255 K ($Zn_{13-\delta 1}Sb_{10}$) and an α′ phase with a slightly lower one, $Zn_{13-\delta 2}Sb_{10}$ ($\delta 1 < \delta < \delta 2$).[9] Because of the difficulty in controlling the initial deficiency δ in the synthesis of Zn_4Sb_3 (i.e., $Zn_{13-\delta}Sb_{10}$), there is scattering in the reported resistivity and thermopower data for this material. The temperature dependence of our data is very similar to that established in a recent investigation by Bhattacharya et al.[28] However, our room-temperature magnitudes are lower (around 108 μV/K and 1.8 mΩ cm instead of 160 μV/K and 3.4 mΩ cm for S and ρ, respectively) and more in agreement with the original values reported in ref 12 (113 μV/K and 2 mΩ cm for S and ρ, respectively).

The resistivity behavior of Zn_4Sb_3 corresponds to that of a poor metal or heavily doped semiconductor. Magnitudes

(27) (a) Pohl, R. O. *J. Non-Cryst. Solids* **2006**, *352*, 3363. (b) Cahill, D. G.; Watson, S. K.; Pohl, R. O. *Phys. Rev. B* **1994**, *46*, 6131.

(28) Bhattacharya, S.; Hermann, R. P.; Keppens, V.; Tritt, T. M.; Snyder, G. J. *Phys. Rev. B* **2006**, *74*, 134108.

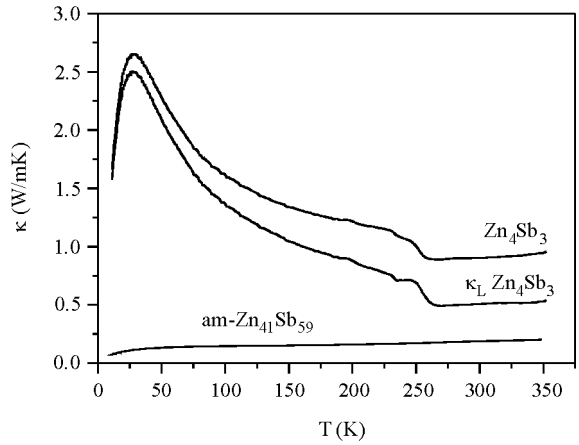

Figure 7. Total thermal conductivity κ of Zn_4Sb_3 and the lattice contribution κ_L compared to the thermal conductivity of am-$Zn_{41}Sb_{59}$.

are in the mΩ cm range and, apart from the discontinuity introduced by the phase transitions, increasing with increasing temperature. This, of course, is radically different to am-$Zn_{41}Sb_{59}$, which is a true semiconductor with resistivity values in the Ω m range. The thermopower of Zn_4Sb_3 is increasing monotonically from 10 K to about 130 K, and then again from 255 to 350 K where the β-phase is stable. The thermopower of am-$Zn_{41}Sb_{59}$ has a similar value as Zn_4Sb_3 at 10 K but increases much faster with increasing temperature.

Figure 7 shows the thermal conductivity of Zn_4Sb_3. Again, the temperature dependence is similar to that reported by Bhattacharya,[28] but as for the resistivity and thermopower we find a lower value at room temperature than these authors (0.9 vs 1.5 W/(m K)), which, however, is in good agreement with the value reported in ref 12. Upon cooling from 350 K, κ decreases slightly until around 255 K, where a discontinuous rise occurs at the $\beta-\alpha$ phase transition. Over the temperature region of the two phase transitions, κ increases by 20−25% which is in agreement with earlier investigations. Upon further cooling, κ rises in a $1/T$ manner until a maximum at around 25 K. This behavior is typical of ordered and well-crystalline materials where heat is carried by elastic waves.[26] The probability of predominant phonon−phonon Umklapp scattering decreases with decreasing temperature, which leads to an increase in the thermal conductivity. The maximum is reached when the phonon mean free path becomes comparable to the crystal dimension.

The lattice contribution to thermal conductivity $\kappa_L = (\kappa - \kappa_e)$ can be assessed from the Wiedemann−Franz relation $\kappa_L = L_O \times 1/\rho \times T$, where $L_O = 2.45 \times 10^{-8}$ V^2/K^2 is the Lorenz number and ρ measured resistivities according to Figures 4 and 6. Because of the high resistivity, the electronic contribution κ_e to the thermal conductivity of am-$Zn_{41}Sb_{59}$ is negligible. This is different for Zn_4Sb_3 and the calculated lattice contribution κ_L has been included in Figure 7. At 350 K, the value of κ_L for disordered β-Zn_4Sb_3 is about 0.6 W/(m K) and decreases to 0.5 W/(m K) at 255 K, where the phase transitions to the ordered phases occur. Thus, the slightly positive temperature dependency seen for κ remains for κ_L and in terms of thermal conductivity β-Zn_4Sb_3 has the characteristics of an amorphous solid. As a matter of fact, the slope $d\kappa/dT$ is virtually identical to that observed for am-$Zn_{41}Sb_{59}$ (c.f. Figure 7). The latter material represents a lower boundary for the lattice thermal conductivity of zinc antimony systems. The magnitudes of κ_L for β-Zn_4Sb_3 between 255 and 350 K are just about three times of those of am-$Zn_{41}Sb_{59}$, i.e., the minimum thermal conductivity in this temperature range.

Similar to clathrates, β-Zn_4Sb_3 can be considered as "phonon-glass" material.[29] Still, the question remains how β-Zn_4Sb_3 realizes phonon-glass behavior. In amorphous materials heat is thought to be transmitted in a random walk from one atom to its nearest and next-nearest neighbors assuming entirely uncorrelated harmonic (Einstein) oscillators.[27] At present, it is debated if the disorder in the crystal structure of β-Zn_4Sb_3 provides effective scattering centers for the heat carrying acoustic phonons, or if a coupling of those with an optic soft mode arising from the rattling of Sb_2 dumbbells is responsible for their efficient scattering.[30]

4. Conclusions

Efficient thermoelectric materials combine low thermal conductivities with good electrical conductivities and the binary intermetallic β-Zn_4Sb_3 exhibits such "phonon-glass electron-crystal" properties. To obtain further insight into the nature of this behavior, we investigated the thermoelectric properties of the bulk amorphous alloy $Zn_{41}Sb_{59}$, which is obtained by high-pressure techniques. A particular chemical system is expected to display minimum thermal conductivity when it is in an amorphous state. In this respect, am-$Zn_{41}Sb_{59}$ should provide a lower boundary for the thermal conductivity of zinc antimony systems. We find that the lattice thermal conductivity of β-Zn_4Sb_3 and the thermal conductivity of am-$Zn_{41}Sb_{59}$ have a very similar temperature dependence in the range 255−350 K and that the magnitudes for crystalline β-Zn_4Sb_3 are just about three times that for the amorphous material. Therefore it appears justified to classify β-Zn_4Sb_3 as a "phonon-glass electron-crystal" material. On the other hand, am-$Zn_{41}Sb_{59}$ does not display "electron-crystal" behavior. Compared to β-Zn_4Sb_3 resistivities are substantially higher and the temperature dependence corresponds to that of a semiconductor. According to Nolas and Goldsmid, amorphous solids may only display useful thermoelectric properties when the effective mass of carriers is large and temperatures are high.[21] Because of its low thermal stability, the condition of high temperature is not applicable for am-$Zn_{41}Sb_{59}$.

Acknowledgment. This work was supported by the ACS Petroleum Research Fund under Grant 45796-AC10. C.N. acknowledges a SUMR fellowship from the ACS Petroleum Research Fund (Grant 45796.01-AC10) and J.N. acknowledges travel grants from the Bengt Lundqvist and K. & A. Wallenberg Foundation.

CM802893V

(29) Cohn, J. L.; Nolas, G. S.; Fessatidis, V.; Metcalf, T. H.; Slack, G. A. *Phys. Rev. Lett.* **1999**, *82*, 779.
(30) Schweika, W.; Hermann, R. P.; Prager, M.; Persson, J.; Keppens, V. *Phys. Rev. Lett.* **2007**, *99*, 125501.